Solar Energy Materials & Solar Cells 141 (2015) 383–390

Contents lists available at ScienceDirect

Solar Energy Materials & Solar Cells

journal homepage: www.elsevier.com/locate/solmat

The effect of nanocrystal reaction time on $Cu_2ZnSn(S,Se)_4$ solar cells from nanocrystal inks

Andrew D. Collord, Hugh W. Hillhouse *

University of Washington, Department of Chemical Engineering, Seattle, WA 98195, USA

ARTICLE INFO

Article history:
Received 22 December 2014
Received in revised form
10 March 2015
Accepted 6 May 2015
Available online 25 June 2015

Keywords:
CZTS
$Cu_2Zn(S,Se)_4$
Solution processing
Nanocrystal
Earth abundant
Kesterite

ABSTRACT

The sintering of nanocrystals to form a bulk film is a promising route for the production of low cost $Cu_2ZnSn(S,Se)_4$ solar cells. However, very little is known about how the synthesis of the nanocrystals impacts the properties of the sintered film or the performance of the resulting photovoltaic device. Here, we present a study in which devices were made from NC inks with different reaction times. Variation in reaction time produces inks with different average size, composition, and compositional heterogeneity. Accounting for the influence of composition, we find that longer NC reaction times result in improved current collection, larger quasi-Fermi level splitting, lower defect concentrations, and higher power conversion efficiency in the selenized devices. The improvements correlate well with the breadth of the x-ray diffraction peaks, suggesting that the longer reaction times result in larger crystalline domain sizes, and that grain boundaries may act as non-radiative recombination sites. Further, the crystalline domain size in the sintered film is proportional to the mean NC size in the ink, suggesting that some interparticle sintering occurs but that the ultimate grain size in the film is dependent on the starting NC size.

1. Introduction

Thin film solar cells based on the earth-abundant Cu_2ZnSnS_4 and $Cu_2ZnSnSe_4$ light absorbing layers, referred to as kesterites, have been the subject of intense research interest in recent years. Due to the high crustal abundance of the constituent elements, and the structural and electronic similarities to $Cu(In,Ga)Se_2$ (CIGSe), kesterites are a leading candidate for terawatt-scale production of photovoltaics. By simply substituting the kesterite absorber into a standard CIGSe device architecture, kesterite solar cells have reached 12.6% efficient [1] using a hydrazine solution process. Another promising route is the sintering of nanocrystal inks. Such devices have reached as high as 9.6% efficient [2] without the use of highly toxic materials. However, the use of colloidal nanocrystals as a precursor to a continuous thin film is still relatively new, and the sintering process in these PV materials has not been thoroughly studied. Strong criteria do not exist for predicting how ligands, particle size, and processing steps impact the resulting films and devices. For example, early attempts to make bulk materials from nanocrystals suggested that the carbonaceous ligands prevented effective sintering [3–5], but more recent work has shown large grained structures [6,7]. Reports have even suggested that the carbonaceous layer commonly observed between the absorber and back contact [8–11] may benefit devices by reducing back contact recombination [9]. To better understand how the properties of the nanocrystals impact the bulk film, we have performed a study in which photovoltaic devices were made from CZTS nanocrystal inks with varying reaction times. These inks vary in average particle size, compositional heterogeneity, and average composition.

2. Materials and methods

2.1. Nanocrystal synthesis

CZTSSe solar cells were made from nanocrystals characterized in detail in a previous publication [12]. Briefly, the nanocrystals are synthesized by injecting a 1 M sulfur in oleylamine solution into a flask containing copper(II) acetylacetonate (Sigma 99.999%), zinc (II) acetylacetonate hydrate (Sigma 99.999%), and tin(IV) bis (acetylacetonate) dichloride (Sigma 98%) in oleylamine (Sigma, technical grade) at 225 °C and allowing the reaction to proceed for a set duration. Following NC synthesis, the reaction mixture is split equally between two centrifuge tubes. From one tube, we precipitate nearly all of the particles (the “All” fraction); from the other we only collect particles above a certain size threshold (the “Standard” fraction). The Standard procedure is the same as was used to produce a 7.2% efficient device [13]. The nanocrystals are

* Corresponding author. Tel.: +1 206 685 5257; fax: +1 206 543 3778.
E-mail address: h2@uw.edu (H.W. Hillhouse).

http://dx.doi.org/10.1016/j.solmat.2015.05.010
0927-0248/

washed multiple times to remove excess oleylamine then dispersed in hexanethiol to form a dense ink.

2.2. Device fabrication

Device fabrication closely follows a previously published method [13]. To deposit films, the NC inks are doctorbladed onto molybdenum coated soda–lime glass then dried on a hot plate at 300 °C in air. Two layers are applied to produce a film that is approximately 1.2 μm thick. The films are then annealed in a graphite box with excess selenium at 500 °C for 20 min to form a polycrystalline CZTSSe film. Following selenization, complete devices are made using standard procedures, including chemical bath deposition of CdS, RF sputtering of i-ZnO then ITO, and thermal evaporation of a Ni/Al top contact. The samples are scribed into devices with a typical area of about 0.45 cm^2.

2.3. Characterization

The composition of the films was measured before and after selenization using energy dispersive spectroscopy (EDS) on a FEI Sirion scanning electron microscope at 20 keV. Completed solar cells are tested under simulated AM1.5G illumination produced using a 300 W Xe arc lamp. The integrated light intensity is validated using a calibrated mono-crystalline Si reference cell. Current–voltage parameters are extracted using the method of Zhang et al. [14]. The external quantum efficiency (EQE) is measured using a lock-in amplifier with monochromatic light, chopped at 153 Hz and the resulting spectrum is integrated over the AM1.5G spectrum and compared to the measured short circuit current. Drive-level capacitance profiling (DLCP) is performed at room temperature using a Solartron SI 1260. The DC peak voltage was varied from −0.5 to +0.5 V with the AC signal ranging from 10 to 300 meV over the frequency range 0.1–46.4 kHz. For determining the defect density, the device was assumed to be a planar one-sided junction and the dielectric constant was assumed to be 8.6 [15]. Absolute intensity photoluminescence (AIPL) spectra are collected on a modified Horiba Labram steady-state PL instrument calibrated using a NIST-calibrated blackbody source. The AIPL spectra are collected over a 110 × 110 μm area using 785 nm laser excitation at approximately 10 suns. A minimum of 6 PL measurements are taken on each sample and the fitted parameters are averaged. The crystallographic structure of the films was analyzed by powder x-ray diffraction (PXRD) using a Bruker D8 Focus with a Cu K-alpha radiation source. The XRD instrumental broadening was measured using a single crystal silicon wafer which had a FWHM of 0.115 2θ, less than half of the narrowest FWHM observed in any of the CZTSSe films.

3. Results and discussion

3.1. Temporal changes to composition

With increasing reaction time we see significant changes in the average composition of both the Standard and All NC inks. As detailed in a previous publication [12] and shown in Fig. 1, the short reaction time inks are extremely Sn-poor, but over time the composition of the inks approaches that of the starting precursors. The NC reaction product contains at least two distinct particle populations: large Zn-rich particles and small Zn-poor particles. Fewer of the small particles are collected in the Standard fraction than in the All ink, causing the All fraction to have higher Cu/(Zn+Sn) ratios and lower Zn/Sn ratios than the Standard fraction. However, because the NC growth mechanism involves the ripening of the small particles into the larger particles, the composition of the All fraction precedes that of the Standard fraction. For example, the Cu/(Zn+Sn) and Zn/Sn ratios for the Standard fraction reacted for 1 h are 0.83 and 1.18; values close to that of the All fraction after only 0.5 h of reaction at 0.83 and 1.22. After about 4 h of reaction nearly all of the particles are collected in the Standard fraction, so the two compositions converge. Comparing the film compositions before and after selenization, we observed that both the Standard and All fraction shift to higher Cu/(Zn+Sn) ratio as a result of both Zn and Sn loss. For reaction times less than 2 h, when the material is very Zn-rich, the shift primarily results from Zn loss, as indicated by a reduction in the Zn/Sn ratio, but for reactions longer than 2 h we also see evidence of Sn loss, as has been documented previously [16–20]. Because ZnS(e) has a very low vapor pressure, the loss of Zn suggests that there is likely unbound (metallic) zinc present during annealing. The elemental losses are significantly lower for the longer reaction times, when the average composition is closer to stoichiometric. Conveniently,

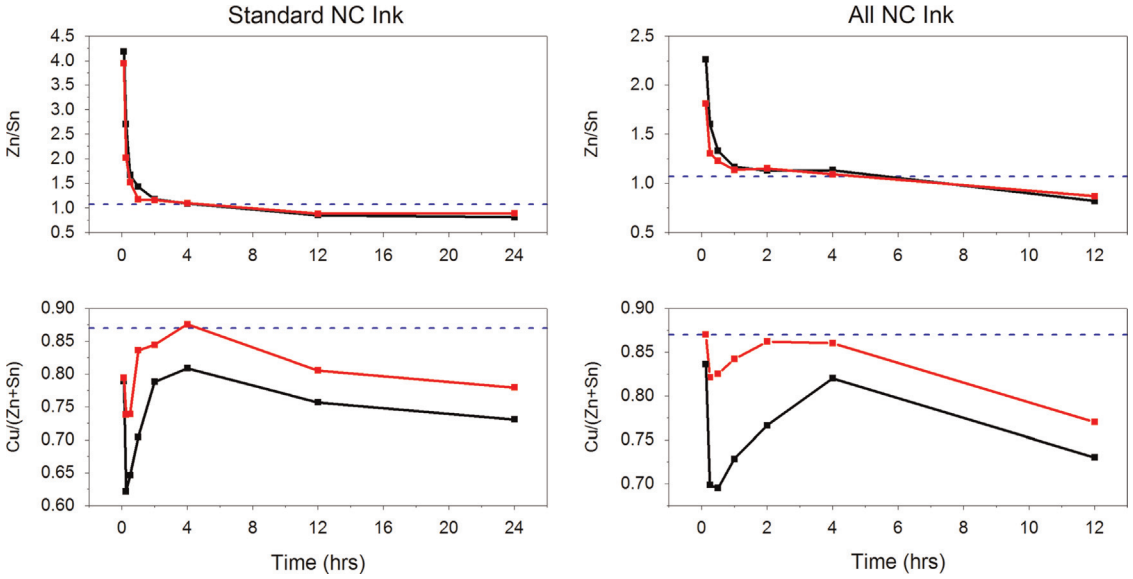

Fig. 1. The change in film composition as a function of time for the (1) "Standard" and (2) "All" particle fractions. Black lines indicate the composition of the doctorbladed film, red lines indicate the composition after selenization. The dashed blue line indicates the ratio of precursors added for NC synthesis. (For interpretation of the references to color in this figure legend, the reader is referred to the web version of this article.)